Chaos synchronization based on a continuous chaos control method in semiconductor lasers with optical feedback

Atsushi Murakami
Department of Electronic Engineering, The University of Electro-Communications, 1-5-1 Chofu-gaoka, Chofu-shi, Tokyo, 182-8585 Japan

Junji Ohtsubo
Faculty of Engineering, Shizuoka University, 3-5-1 Johoku, Hamamatsu, 432-8561 Japan
(Received 28 August 2000; published 14 May 2001)

Chaos synchronization using a continuous chaos control method was studied in two identical chaotic laser systems consisting of semiconductor lasers and optical feedback from an external mirror. Numerical calculations for rate equations indicate that the stability of chaos synchronization depends significantly on the external mirror position. We performed a linear stability analysis for the rate equations. Our results show that the stability of the synchronization is much influenced by the mode interaction between the relaxation oscillation frequency of the semiconductor laser and the external cavity frequency. Due to this interaction, an intensive mode competition between the two frequencies destroys the synchronization, but stable synchronization can be achieved when the mode competition is very weak.

DOI: 10.1103/PhysRevE.63.066203 PACS number(s): 05.45.Xt, 42.65.Sf, 05.45.Gg, 05.45.Pq

I. INTRODUCTION

Synchronization of coupled nonlinear oscillators has been of great interest. It is a ubiquitous phenomenon and is often observed in physical and biological fields [1]. In particular, during the last decade, much interest in the phenomena of the synchronized chaotic behavior of coupled nonlinear systems has developed since the concept of chaos synchronization was first reported by Pecora and Carroll in 1990 [2]. Chaos synchronization has a high potential for application to secure communications. Although secure communications has been demonstrated in a simple, low-dimensional chaotic system [3], it was later realized that a sufficient level of security could not be ensured in such a simple system [4]. A time-delay system is a good candidate for highly secure communications based on synchronized chaotic systems because of its ability to generate high-dimensional chaos [5].

Implementation of secure communications on an optical system has also become a very interesting issue with the recent rapid development of optical-fiber communications. Laser sources generating chaos are required for such optical secure communication systems. Many researchers have already investigated the chaotic behavior and physical mechanisms in several laser systems [6–12]. In recent years, chaos synchronization has been experimentally and theoretically investigated in laser systems such as Nd:YAG lasers, CO_2 lasers, erbium-doped fiber ring lasers, and NH_3 lasers [13–17]. Furthermore, several demonstrations of secure communications based on such synchronized lasers have been reported, and the possibility of the practical application of optical secure communications has been suggested [18–21].

There are many kinds of lasers, but semiconductor lasers are the most attractive and important source generators in optical secure communications because they have already been used in optical-fiber communications. Recently, an experiment on secure communications using semiconductor laser chaos was carried out by Geodgebuer *et al.* [22]. They used a nonlinear optical component in an optoelectric feedback loop to generate the submicrosecond chaotic fluctuation. The bandwidth of the message signal in this system was a few kilohertz. In contrast, a much faster chaotic oscillation can be obtained from direct optical feedback from an external mirror. In this case, the chaotic oscillation reaches the subnanosecond time scale. Several theoretical and experimental studies on synchronization and secure communications using the optical-feedback-induced chaos have already been conducted [23–29]. However, Pecora and Carroll's method is not suited for chaos synchronization in this case because it requires dividing a chaotic system into two subsystems [21]. Therefore, a configuration of unidirectional light injection from a chaotic master to solitary slave lasers was used [21,30,31,25–28]. Similar chaotic outputs are observed between the two lasers in such a configuration. In this case, however, it is unclear whether chaotic outputs come from a light amplification of the master's chaotic emission through injection locking or a principle of chaos synchronization [21,27,28].

Another practical technique for chaos synchronization was proposed by Pyragas in 1993 [32]. He applied continuous chaos control to chaos synchronization. This method is very well suited for synchronizing two identical chaotic systems[33]. Recently, this method was also applied to time-delay systems, where it was analytically shown that stable synchronization could be achieved [6,34]. In this paper, we apply a continuous chaos control method to synchronize two identical chaotic systems consisting of a semiconductor laser and a delayed optical feedback. Feedback-induced optical chaos and synchronization in semiconductor lasers may facilitate optical secure communications with a high level of security. We performed a numerical simulation and linear stability analysis for the rate equations and investigated the physical properties and stability for chaos synchronization in this case.

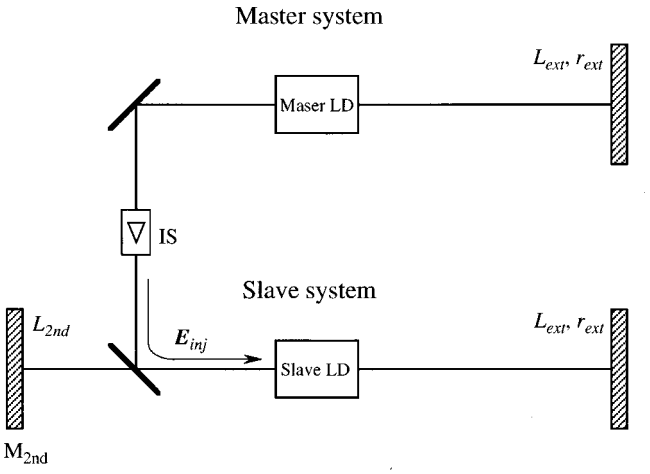

FIG. 1. Optical setup for chaos synchronization based on a semiconductor laser with optical feedback from an external mirror. Unidirectional coupling from the master to slave system is provided by an optical isolator (IS). Second mirror M_{2nd} is inserted in the slave system to provide negative feedback to the slave laser.

II. MODEL AND RATE EQUATIONS

Here we briefly review the synchronization scheme proposed by Pyragas. We consider two identical time-delay feedback systems with the delay time τ coupled in a driver-response scheme as follows [5]:

$$\dot{x}=f(x,x_\tau) \quad [x_\tau := x(t-\tau),\ f \ \text{continuous}], \tag{1}$$

$$\dot{y}=f(y,y_\tau)+K(x-y). \tag{2}$$

The term $K(x-y)$ in Eq. (2) represents dissipative coupling [34], which leads to a continuous chaos control with coupling strength K. The two systems are synchronized when the difference in outputs always has a fixed zero value. The condition $x=y$ is usually called the ''synchronization manifold.'' If the two outputs become slightly different, negative feedback always can restore the two systems to the synchronization manifold. Therefore, stable synchronization can be achieved.

Next, we apply the synchronization scheme to a semiconductor laser with optical feedback. The optical setup for chaos synchronization is shown in Fig. 1. The master and slave systems are identical and are composed of a semiconductor laser and an external mirror. $L_{\rm ext}$ and $r_{\rm ext}$ represent the external cavity length, defined as the distance from the laser exit facet to the external mirror, and the amplitude reflectivity of the external mirror. Here we assume that the amplitude reflectivity corresponds to the optical feedback rate injected into the active layer of the semiconductor laser. The output of the master laser is unidirectionally injected into the slave laser via the optical isolator (IS). A second external mirror ($M_{2\rm nd}$) of external cavity length $L_{2\rm nd}$ is introduced to apply a second optical feedback loop to the slave laser. The injected light from the master laser and the second optical feedback light can provide a continuous chaos control to the slave system, leading to synchronization.

Mathematical expressions in our system are based on the well-known Lang-Kobayashi rate equations [6], which give a valid approximation for a single-mode semiconductor laser with weak to moderate optical feedback from an external mirror. The rate equations of the complex electric field and the carrier density for the master and the slave lasers are given by

$$\frac{dE_m(t)}{dt}=\frac{1}{2}(1+i\alpha)\{G_N[N_m(t)-N_0]-\gamma_c\}E_m(t) + \kappa E_m(t-\tau)e^{-i\omega_0\tau}, \tag{3}$$

$$\frac{dE_s(t)}{dt}=\frac{1}{2}(1+i\alpha)\{G_N[N_s(t)-N_0]-\gamma_c\}E_s(t) + \kappa E_s(t-\tau)e^{-i\omega_0\tau} + K[E_{\rm inj}(t)+E_s(t-\tau_{2nd})e^{-i\omega_0\tau_{2\rm nd}}], \tag{4}$$

$$\frac{dN_{m,s}(t)}{dt}=J-\gamma_N N_{m,s}(t)-G_N[N_{m,s}(t)-N_0]|E_{m,s}(t)|^2, \tag{5}$$

where the subscripts m and s correspond to the master and slave lasers. The equations for the carrier density have the same form for the two lasers. α is the linewidth enhancement factor, G_N is the linear gain coefficient, γ_c is the cavity decay rate, γ_N is the carrier decay rate, N_0 is the carrier density at transparency, and J is the injection current density. For the master laser, the second term on the right-hand side of Eq. (3) accounts for the optical feedback effect. $\kappa=(1-r_0^2)r_{\rm ext}/r_0/\tau_{\rm in}$ represents the feedback strength, where r_0 is the amplitude reflectivity of the laser exit facet and τ_{in} is the round-trip delay time within the laser cavity. $\tau=2L_{\rm ext}/c$ represents the round-trip delay time within the external cavity, where c is the velocity of light in vacuum. $\omega_0\tau$ is the round-trip phase shift generated in the light propagation within the external cavity, where ω_0 is the angular frequency of the solitary laser. The dissipative coupling between the two laser outputs is presented in the third term on the right-hand side of Eq. (4), and the coupling strength is denoted by $K=(1-r_0^2)k_{\rm cp}/r_0/\tau_{\rm in}$, where $k_{\rm cp}$ is the coupling rate. In the coupling term, $E_{\rm inj}(t)=E_m(t)$ and $\tau_{2\rm nd}=2L_{2\rm nd}/c$. To produce a continuous chaos control by the second mirror, we set the mirror position to $L_{2\rm nd}=L_{\rm ext}\pm\lambda/4$ (λ being the wavelength of the solitary laser). The round-trip phase shift for the second external cavity becomes $\omega_0\tau_{2\rm nd}=\omega_0\tau\pm\omega_0\lambda/(2c)$. Using $\lambda=2\pi c/\omega_0$, we obtain $\omega_0\tau_{2\rm nd}=\omega_0\tau\pm\pi$. The round-trip times for the original and second external mirror are approximately equal, i.e., $\tau_{2\rm nd}\approx\tau$. Consequently, the coupling of the optical feedback from the second external mirror becomes negative relative to that from the original feedback, i.e., $E_s(t-\tau_{2\rm nd})\exp(-i\omega_0\tau_{2\rm nd})\approx -E_s(t-\tau)\exp(-i\omega_0\tau)$. We call this ''negative optical feedback'' in the following. We mention again that the relation $\omega_0\tau_{2\rm nd}=\omega_0\tau\pm\pi$ is the required condition for continuous chaos control.

Assuming the complex electric field to be $E(t)=E_0(t)\exp[i\phi(t)]$, we obtain a complete set of rate equations

TABLE I. Parameter values for the rate equations based on Al_xGaAs_{1-x} CSP semiconductor lasers.

Symbol	Parameter	Value
G_N	Gain coefficient	$8.4\times10^{-13}\,m^3\,s^{-1}$
α	Linewidth enhancement factor	3
r_0	Facet amplitude reflectivity	0.556
N_{th}	Carrier density at threshold	$2.018\times10^{24}\,m^{-3}$
N_0	Carrier density at transparency	$1.4\times10^{24}\,m^{-3}$
τ_s	Carrier lifetime	2.04 ns
τ_p	Photon lifetime	1.927 ps
τ_{in}	Round-trip time in the laser cavity	8 ps
V	Active region volume	$6.96\times10^{-17}\,m^3$
λ	Wavelength	800.0 nm
α_m	Facet loss	$35\ cm^{-1}$
μ_g	Group refractive index	4

for the field amplitude, phase, and carrier density. We perform numerical simulations based on these rate equations by employing a fourth-order Runge-Kutta algorithm. Langevin noise and other noise must be taken into account in actual semiconductor lasers. However, we do not consider these noises because we treat only deterministic dynamics in this paper. Laser parameter values used in our investigation are based on $Al_xGa_{1-x}As$ CSP semiconductor lasers with a wavelength of 800.0 nm, as listed in Table I. In the numerical simulation, we chose a condition $\omega_0\tau_{2nd}=\omega_0\tau+\pi$ for setting the second mirror position. The following presents fundamental characteristics of the feedback-induced chaos and discusses chaos synchronization of the two semiconductor lasers.

III. BIFURCATION OF SEMICONDUCTOR LASERS WITH OPTICAL FEEDBACK

Before considering the synchronization problem, we will present the fundamental characteristics of the optical feedback system. In a semiconductor laser with optical feedback, the laser output exhibits a bifurcation route to chaos with an increase of the feedback strength. The relaxation oscillation and external cavity frequencies play key roles in the bifurcation scenario. The former is the dominant oscillation mode of a solitary semiconductor laser, and the latter is the frequency determined by the round-trip time of light propagation within the external cavity. A typical bifurcation sequence with optical feedback is as follows. In the absence of feedback, the laser output exhibits constant intensity after the relaxation oscillation. However, when the laser is subjected to optical feedback, the relaxation oscillation becomes undamped and the stable output intensity evolves into a periodic oscillation at the frequency of the relaxation oscillation. This is called ''Hopf bifurcation'' [7,11]. As the optical feedback is increased, the external cavity frequency is excited and laser output exhibits higher-order periodic or quasiperiodic oscillations. Finally, the laser reaches the chaotic state at a sufficient level of optical feedback.

In the bifurcation route, the mode interaction between the relaxation oscillation and external cavity frequencies is a very important factor because it changes bifurcation stability. This has already been demonstrated both theoretically and experimentally [8,9]. Here we briefly explain it. For example, Fig. 2 is a phase diagram showing a boundary of the Hopf bifurcation as a function of the amplitude reflectivity and the external cavity length for the external mirror, at an injection current $J=1.3J_{th}$. The round-trip phase was set to 2π. The laser output below the boundary has a stable fixed state. In this case, the relaxation oscillation frequency is $f_R=2.5\,GHz$. We can see that the boundary has a periodic structure along L_{ext}. The external cavity frequency f_{ext} changes for variations of L_{ext}. When the relaxation oscillation frequency f_R becomes close to the external cavity frequency or a harmonic of it, namely, $f_R\approx m f_{ext}$ (m being integer), an intensive mode competition between the two frequencies occurs. An external cavity mode suppresses the excitation of the relaxation oscillation. Consequently, the Hopf-bifurcation boundary exhibits local peaks as shown in the figure. For example, we see a model of this kind of bifurcation in Fig. 5(a), below. We call this bifurcation ''unstable bifurcation'' in the following. In contrast, the bifurcation sequence is relatively smooth at the external cavity lengths around the valleys of Fig. 2 because the mode competition is so weak that the relaxation oscillation can easily be excited. We call this kind of bifurcation ''stable bifurcation'' in the following. We expect that the synchronization characteristic is also different for these stable and unstable bifurcations. In the next section, we present numerical results of the synchronization for an external cavity length of $L_{ext}=15\,cm(12\,cm)$, corresponding to the valley (peak) in Fig. 2.

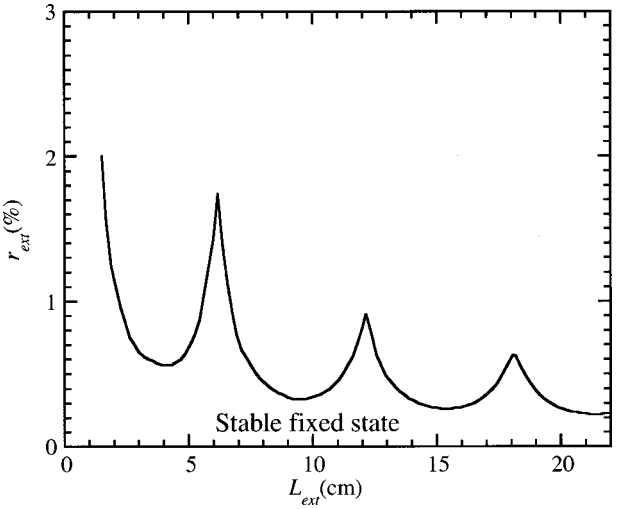

FIG. 2. Phase diagram for stability in semiconductor laser with a single external mirror as a function of amplitude reflectivity and external cavity length for the external mirror. Feedback phase for the external cavity length is always fixed to be 2π.

IV. SYNCHRONIZATION

We will first present an example of synchronizing chaotic state for a stable bifurcation. Figures 3(a) and 3(b) show the

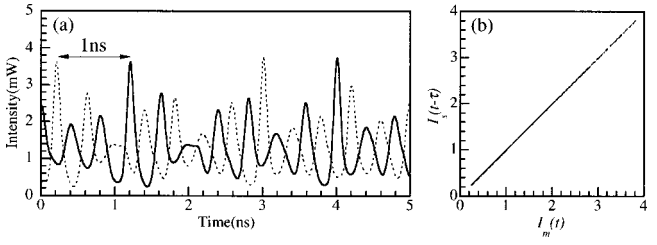

FIG. 3. Synchronized chaotic wave forms. The solid (dashed) curve represents chaotic output from the master (slave) system. Parameter values are $J=1.3J_{\rm th}$, $L_{\rm ext}=15\,{\rm cm}$, $r_{\rm ext}=1.3\%$, and $k_{\rm cp}=1.0\%$. The time lag between them is 1 ns, corresponding to the external delay time $\tau=2L_{\rm ext}/c$. Thus the synchronization manifold is $x_m(t)=x_s(t-\tau)$ ($x=E$, ϕ, and N).

chaotic temporal wave forms and the correlation plots for the output intensities of the master and slave lasers. The output intensity was calculated as $I=[hc\omega\alpha_m V/(4\pi\mu_g)]E^2$[23]. The parameter values are the injection current of $J=1.3J_{\rm th}$, the external cavity length of $L_{\rm ext}=15\,{\rm cm}$, the external reflectivity of $r_{\rm ext}=1.3\%$, and the coupling rate of $k_{\rm cp}=1.0\%$. In Fig. 3(a), the solid (dashed) line represents the chaotic output intensities of the master (slave) laser. It is explicitly shown that there is a 1-ns time lag for the synchronization, which is identical to the delay time τ. Therefore, the synchronization manifold is given as $I_m(t)=I_s(t-\tau)$. This is called ''anticipating synchronization,'' which can be seen in synchronization for time-delay systems [34]. In this case, the slave system always anticipates future states of the master system's behavior. In Fig. 3(b), the linear correlation between the two outputs demonstrates that good synchronization is achieved. We introduce here a synchronization error, which is defined as $\sigma=\langle|I_m(t)-I_s(t-\tau)|\rangle/\langle I_m(t)\rangle$ where $\langle\cdots\rangle$ denotes the time average [28]. We define a critical error for good synchronization as $\sigma\leqslant 5\%$. We investigated synchronization for various master system outputs with different values of $r_{\rm ext}$. Figure 4 shows an example of a bifurcation diagram in the master system and a corresponding synchronization region in the slave system. Figure 4(a) shows a quasiperiodic route to chaos with increases of $r_{\rm ext}$. It should be noted that it is a stable bifurcation. Figure 4(b) represents an interval of $k_{\rm cp}$ corresponding to the synchronization as a function of $r_{\rm ext}$ for $\sigma\leqslant 5\%$. The solid line denotes the relation of $k_{\rm cp}=r_{\rm ext}$. We see a wide region for the synchronized state when the coupling rate is smaller than the feedback rate. The chaos synchronization is seen in the range of $r_{\rm ext}=1.15\%-1.50\%$. For a high feedback level, the two lasers can no longer synchronize. We can consider that strong feedback degrades the laser coherence, leading to a loss of synchronization with decreased efficiency of continuous chaos control. Here we mention the synchronization condition of $k_{\rm cp}=r_{\rm ext}$, denoted by the solid line in the figure. Under this condition, the optical feedback effects of the two mirrors in the slave system are compensated for. The slave system behaves like a simple, solitary laser injected only by the output of the master laser. Therefore, much more stable synchronization is expected.

Another synchronization result, which corresponds to an unstable bifurcation, is shown in Fig. 5. The external cavity

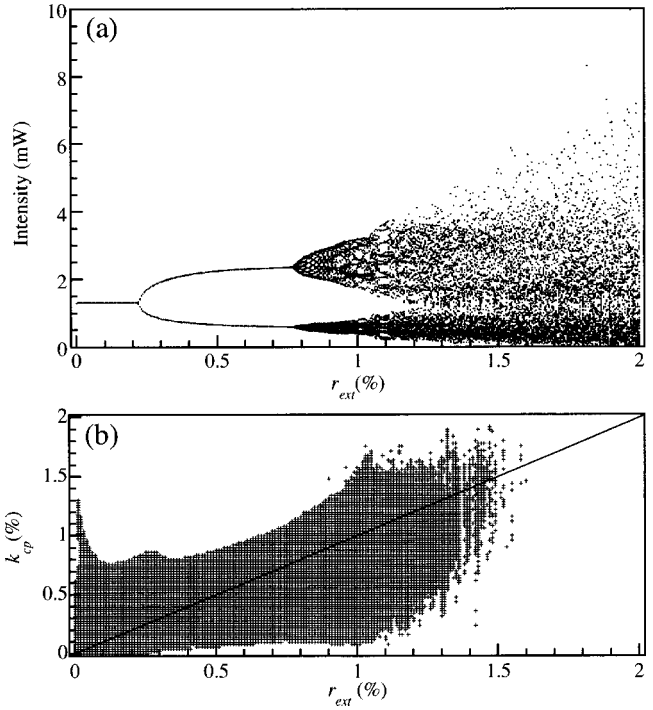

FIG. 4. (a) Bifurcation diagram of the master system with increased feedback. (b) Region of the coupling rate corresponding to the synchronized slave system. Parameter values are $J=1.3J_{\rm th}$ and $L_{\rm ext}=15\,{\rm cm}$. The external cavity length corresponds to a stability bottom, which provides a stable bifurcation. The solid line in (b) represents the relation of $k_{\rm cp}=r_{\rm ext}$.

length is $L_{\rm ext}=12\,{\rm cm}$. The obtained result somewhat differs from that in Fig. 4 in that most of the synchronization region is below the condition of $k_{\rm cp}=r_{\rm ext}$. It is difficult to obtain a synchronized chaotic state for such an unstable bifurcation. Even for the periodic state, the synchronization tends to be lost before the coupling rate reaches the feedback rate. These observations will be discussed in the next section.

V. STABILITY OF SYNCHRONIZATION

In this section, we analytically examine the stability of chaos synchronization based on a linear stability analysis for the rate equations and discuss the numerical results. Mathematically, linear stability analysis is limited for direct application to dynamic behavior because of its linearization in the analysis. However, the analysis is a useful tool for obtaining physical insight into the dynamic behavior of a semiconductor laser with optical feedback [8]. In the following, we investigate the stability of synchronization of the two systems in their fixed states very close to a Hopf-bifurcation point.

We assume a synchronization manifold as the stationary state of the two lasers, i.e., $E_m(t)=E_s(t)=E_{\rm st}$, $\phi_m(t)=\phi_s(t)=\phi_{\rm st}(t)=(\omega_{\rm st}-\omega_0)t$, and $N_m(t)=N_s(t)=N_{\rm st}$. A slight deviation from the synchronization manifold is considered in the slave system, such as $x_s(t)=x_{\rm st}+\delta x(t)$ ($x=E$, ϕ, and N). Here the deviation is defined as an exponential perturbation in the form of $\delta x(t)=\delta x_0\exp(st)$, where $s=\gamma+i\omega$ is a complex parameter, referred to as the ''linear mode.'' γ and ω represent the decay rate and oscillation

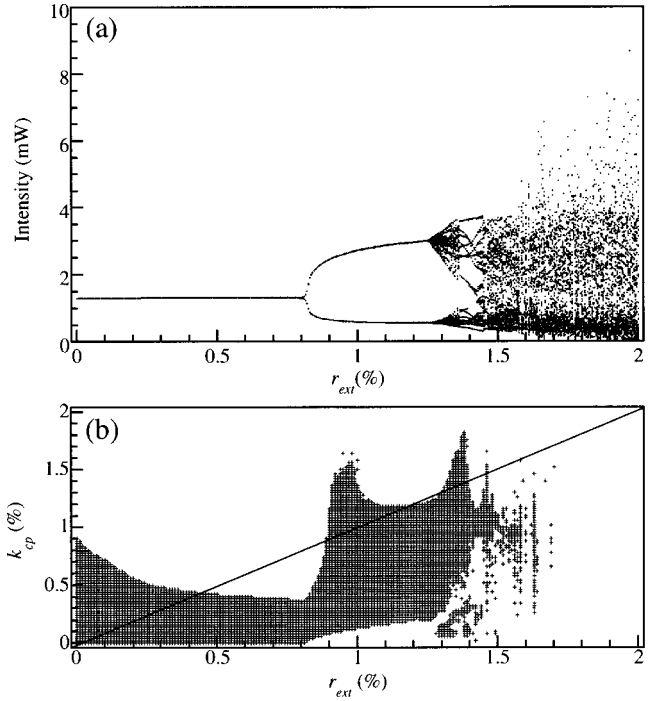

FIG. 5. (a) Bifurcation diagram of the master system. (b) Synchronization region for the coupling rate at $J=1.3J_{\mathrm{th}}$ and $L_{\mathrm{ext}}=12$ cm. The external cavity length corresponds to a stability peak, which provides an unstable bifurcation. The solid line in (b) also shows the relation of $k_{\mathrm{cp}}=r_{\mathrm{ext}}$.

frequency of the linear mode. Therefore, it follows that the synchronization is stable for a linear mode with a negative value of γ because of its exponential decrease with time. In contrast, the slight deviation diverges and the synchronization is lost when a linear mode has a positive γ. Here $\gamma=0$ represents a boundary of the stability for synchronization. Substituting all the assumptions into Eqs. (3)–(5) leads to linearized equations for the perturbation $\delta x(t)$. We then obtain a characteristic equation for the stability of the synchronization (see the Appendix for the detailed derivation). Calculating the characteristic equation, we have a large number of linear modes as a solution. In general, a linear mode distribution can vary depending on the system's condition, which leads to interaction and competition among linear modes. It is possible to experimentally investigate these phenomena by observing the optical spectra of laser outputs [9]. In the following, we present the distribution and transition of the linear modes to discuss the stability of the synchronization for stable and unstable bifurcation sequences.

Figure 6 illustrates linear mode transitions with changes of the coupling between the two systems. It corresponds to the numerical results for the stable bifurcation shown in Fig. 4. The parameter values are $J=1.3J_{\mathrm{th}}$, $L_{\mathrm{ext}}=15$ cm, and $r_{\mathrm{ext}}=0.26\%$. Note that they correspond to the Hopf-bifurcation point in Fig. 4(a). The horizontal and vertical axes represent the real and imaginary parts of s. Synchronization stability with linear mode transitions differs in the coupling ranges of $k_{\mathrm{cp}}<r_{\mathrm{ext}}$ and $k_{\mathrm{cp}}>r_{\mathrm{ext}}$. We present the results for the former and latter cases in Figs. 6(a) and 6(b). In Fig. 6(a), the circles represent linear modes without coupling $k_{\mathrm{cp}}=0\%$. Here X is the mode distribution at $k_{\mathrm{cp}}=r_{\mathrm{ext}}=0.26\%$. The gray dots represent loci of the mode transition for $0<k_{\mathrm{cp}}<0.26\%$. Mode A is a linear mode having the highest value of γ and is located near the relaxation oscillation frequency of the solitary laser (2.5 GHz at $J=1.3J_{\mathrm{th}}$ in this case). All of the other stable modes originate from the external cavity frequency and its harmonics. In the absence of coupling, mode A is an unstable solution for synchronization because the real part is located on the $\gamma=0$ axis, while the other modes are stable solutions. When the two systems are coupled, mode A becomes stable so that the two systems synchronize. The mode transition explicitly shows that the stability of the synchronization is increased as the coupling rate increases. In contrast, for $k_{\mathrm{cp}}>r_{\mathrm{ext}}$, the stability decreases with increased coupling, as shown in Fig. 6(b). One can see that the mode competition between modes A and B occurs around the relaxation oscillation frequency. Finally, the synchronization is destroyed when mode C becomes un-

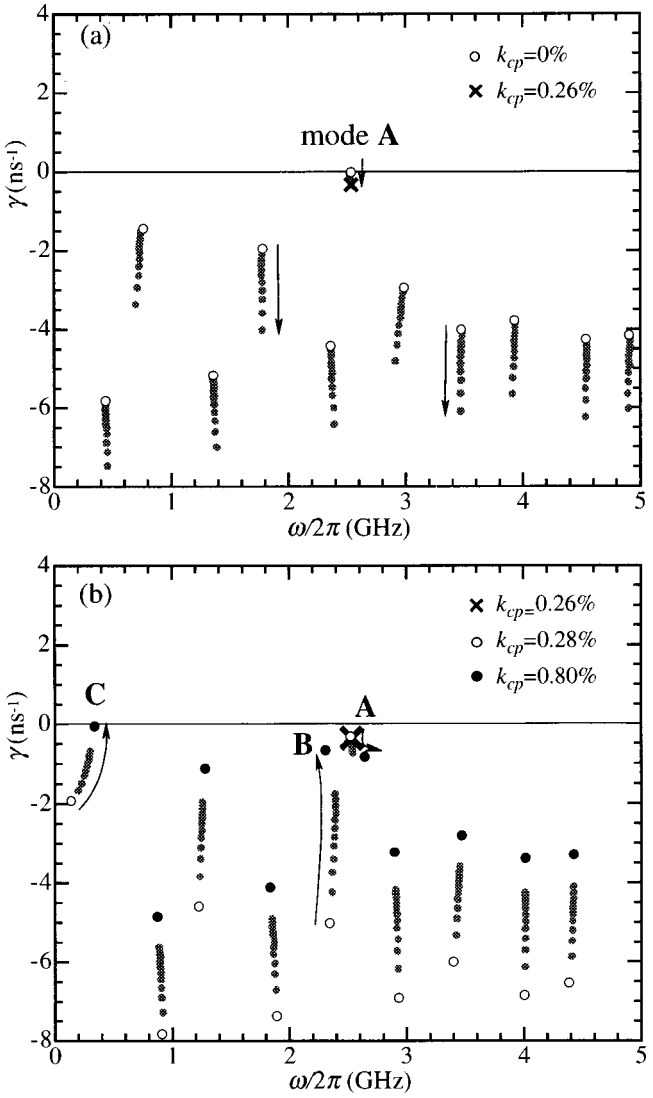

FIG. 6. Distribution and transition for the linear mode with increased coupling rate for stable bifurcation. Parameter values, are $J=1.3J_{\mathrm{th}}$ $L_{\mathrm{ext}}=15$ cm, and $r_{\mathrm{ext}}=0.26\%$. The value of k_{cp} is varied (a) 0–0.26% and (b) 0.26%–0.8%.

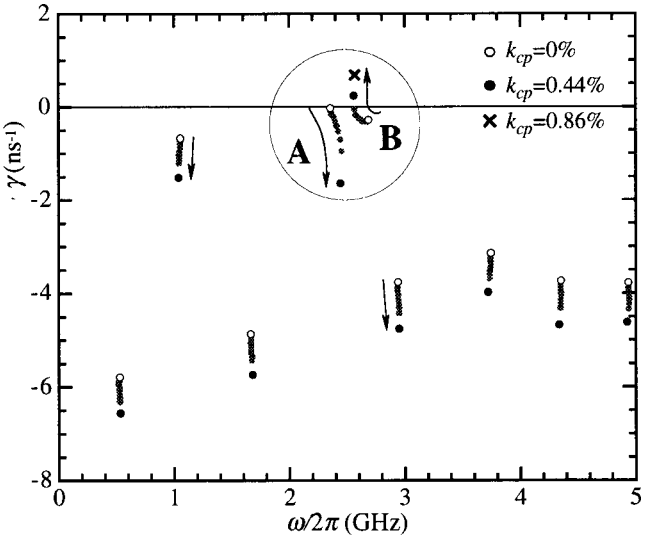

FIG. 7. Distribution and transition for the linear mode with increased coupling rate for unstable bifurcation. Parameter values are $J=1.3J_{\mathrm{th}}$, $L_{\mathrm{ext}}=12$ cm, and $r_{\mathrm{ext}}=0.86\%$. Here k_{cp} is varied 0–0.86%.

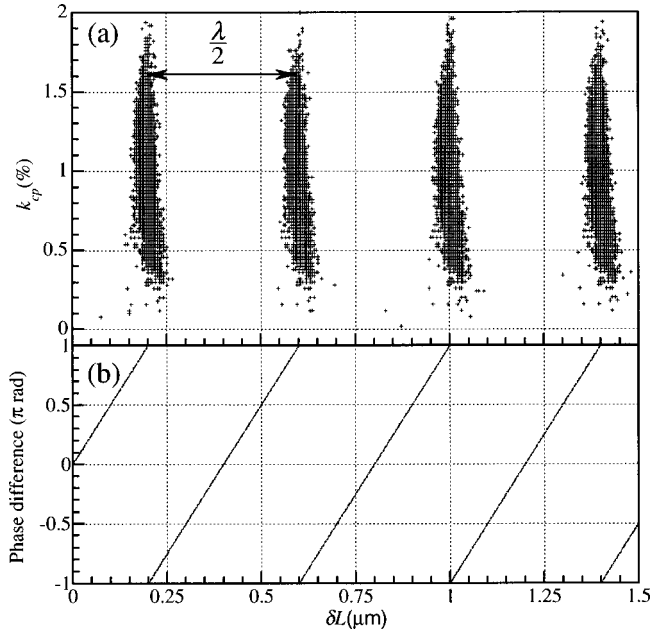

FIG. 8. (a) Synchronization region as a function of $L_{2\mathrm{nd}}$ and k_{cp}. Here $L_{2\mathrm{nd}}$ is slightly changed from 15.0 cm to 15.0 cm+1.5 μm. The other parameter values are $J=1.3J_{\mathrm{th}}$, $L_{\mathrm{ext}}=15$ cm, and $r_{\mathrm{ext}}=1.2\%$. (b) Variation in the round-trip phase difference $\omega_0\tau_{2\mathrm{nd}}-\omega_0\tau$ with a change of $L_{2\mathrm{nd}}$.

stable at $k_{\mathrm{cp}}=0.80\%$. These two figures reveal that the interval of k_{cp} corresponding to the synchronization is 0.8%, which coincides with the numerical result shown in Fig. 4. We can see a special case of stability at $k_{\mathrm{cp}}=r_{\mathrm{ext}}$, which corresponds to the boundary between the two coupling ranges. Under this condition, there exists only one stable mode, the relaxation oscillation mode. All of the other external cavity modes from optical feedback are eliminated. This is because the two optical feedbacks in the slave system compensate for each other so that the slave system seems like a simple, solitary laser injected only by the master laser output. The mode distribution, denoted by *X*, implies that this condition can provide stable synchronization without any mode competition. It is also interesting that the situation is the same as a synchronization configuration based on injection locking, which several researchers used in their experiments in Refs. [21], [26–28]. An injection-locking scheme can be considered as a special case of our configuration. It is beyond the scope of this paper to discuss whether or not the injection-locking scheme corresponds to the synchronization scheme using continuous chaos control. However, we will mention that optical injection from a chaotic master into solitary slave lasers is one configuration for achieving stable chaos synchronization in laser systems.

We show another result of the linear stability analysis in Fig. 7. The figure is the result for an unstable bifurcation corresponding to the numerical result shown in Fig. 5. The two lasers are set to their fixed states close to a Hopf-bifurcation point in Fig. 5(b). The parameter values are $J=1.3J_{\mathrm{th}}$, $L_{\mathrm{ext}}=12$ cm, and $r_{\mathrm{ext}}=0.86\%$. A mode transition with increased coupling differs somewhat from that for the stable bifurcation. In Fig. 7, the white circles are linear modes without the coupling. There are two modes *A* and *B* near the relaxation oscillation frequency. These two modes originate from the relaxation oscillation frequency and the external cavity frequency. Mode competition between the two modes occurs with the coupling. Mode *A* becomes much more stable, while mode *B* becomes unstable as the coupling rate increases. Consequently, the synchronization is lost when mode *B* reaches the $\gamma=0$ axis at $k_{\mathrm{cp}}=0.3\%$. The interval of k_{cp} for synchronization is 0.3%, which also agrees well with the numerical result in Fig. 5.

VI. DISCUSSION

From an experimental point of view, it is difficult to set the position of the second external mirror so that the condition $L_{2\mathrm{nd}}=L_{\mathrm{ext}}\pm\lambda/4$ is satisfied. For that reason, we investigated the sensitivity of chaos synchronization to a small variation of the second mirror position around the required condition. We show the result in Fig. 8(a). The synchronized chaotic state is the same as that in Fig. 3. We varied the external cavity length for the second mirror from 15.0 cm to 15.0 cm+1.5 μm. As a result, we could see several separated regions along the variation in the second mirror position with a period equal to half of the optical wavelength (=0.40μm) [10]. Figure 8 shows the difference in the round-trip phase shift between the second and the original external mirrors, which was calculated as $\omega_0\tau_{2\mathrm{nd}}-\omega_0\tau$. It is explicitly shown that the phase difference is linearly changed between $-\pi$ and π for variation in the second mirror position. Comparing these two figures, we found a correspondence between the synchronization region and phase difference of $\pm\pi$. Note that the phase difference corresponds to the required condition for continuous chaos control. However, it should also be noted that the second external cavity length has to be restricted to within $\tau_{2\mathrm{nd}}\approx\tau$, as already mentioned in Sec. II.

VII. CONCLUSIONS

We have investigated chaos synchronization and its stability in two chaotic laser systems based on a semiconductor laser with optical feedback. The chaos synchronization scheme using continuous chaos control proposed by Pyragas was applied to our case. The two systems are optically coupled by light injection from the master to slave lasers. In order to achieve continuous chaos control, we introduced a second external mirror to the slave system. The position of the second external mirror was adjusted so that the round-trip phase was shifted by π relative to that for the original external mirror in the slave system. Consequently, the second external mirror can provide negative optical feedback relative to the original optical feedback, which leads to continuous chaos control.

We performed numerical simulations for the rate equations and presented the parameter regions corresponding to the chaos synchronization. Based on the numerical results, we applied linear stability analysis to the rate equations around the Hopf-bifurcation points. By investigating the distribution and transition of the linear modes, we obtained several properties for synchronization stability. Consequently, we found that mode interactions between the relaxation oscillation and external cavity frequencies affect the synchronization stability. Stable synchronization can be achieved when the mode competition between the two frequencies is relatively weak. However, synchronization can be easily lost due to the intensive mode competition between the two frequencies. In particular, we found that there is no mode competition when the coupling rate is identical to the feedback rate. Under this condition, all of the external cavity modes are eliminated in the slave system, and we expect stable synchronization in this case.

Finally, we discussed these results from the practical point of view. We investigated chaos synchronization for slight variations in the second mirror position on the order of the optical wavelength. As a result, we found the sensitivity of synchronization to the round-trip phase shift for the second external mirror.

ACKNOWLEDGMENTS

The authors would like to thank Professor K. Atsuki, Dr. Y. Liu, Dr. A. Uchida, and Y. Takiguchi for valuable discussions.

APPENDIX

In this appendix, we perform a linear stability analysis of the synchronization around the stationary state. At synchronization manifold, the mathematical expressions for the two systems are identical. In this condition, rate equations for the amplitude, phase, and carrier density are written as follows [6–8]:

$$\dot{E}(t)=\frac{1}{2}\{G_N[N(t)-N_0]-\gamma_c\}E(t)+\kappa E(t-\tau)\times\cos[\phi(t)-\phi(t-\tau)+\omega_0\tau], \tag{A1}$$

$$\dot{\phi}(t)=\frac{\alpha}{2}\{G_N[N(t)-N_0]-\gamma_c\}-\kappa\frac{E(t-\tau)}{E(t)}\sin[\phi(t)-\phi(t-\tau)+\omega_0\tau], \tag{A2}$$

$$\dot{N}(t)=J-\gamma_N N(t)-G_N[N(t)-N_0]E(t)^2. \tag{A3}$$

Let us assume stationary states as their synchronization manifold. Substituting $E(t)=E_{st}$, $\phi(t)=(\omega_{st}-\omega_0)t$, and $N(t)=N_{st}$ into Eqs. (A1)–(A3), the stationary solutions are given by the following equations:

$$E_{\rm st}=\frac{J-\gamma_N N_{\rm st}}{G_N(N_{\rm st}-N_0)}, \tag{A4}$$

$$\omega_{\rm st}-\omega_0=\kappa[\alpha\cos(\omega_{\rm st}\tau)+\sin(\omega_{\rm st}\tau)], \tag{A5}$$

$$N_{\rm st}=N_0+\frac{\gamma_c-2\kappa\cos(\omega_{\rm st}\tau)}{G_N}. \tag{A6}$$

In the slave system, assuming exponential perturbation from the synchronization manifold, such as $x_s(t)=x_{\rm st}+\delta x_0\exp(st)$ ($x=E$, ϕ, and N), we obtain the following linearized equations for the perturbations in matrix form:

$$\begin{pmatrix} s+\zeta\cos(\omega_{\rm st}\tau) & \zeta E_{\rm st}\sin(\omega_{\rm st}\tau) & -\frac{1}{2}G_N E_{\rm st} \\ -\zeta\frac{\sin(\omega_{\rm st}\tau)}{E_{\rm st}} & s+\zeta\cos(\omega_{\rm st}\tau) & -\frac{\alpha}{2}G_N \\ 2G_N E_{\rm st}(N_{\rm st}-N_0) & 0 & s+\gamma_N+G_N E_{\rm st}^2 \end{pmatrix} \times\begin{pmatrix}\delta E_0\\ \delta\phi_0\\ \delta N_0\end{pmatrix}=0, \tag{A7}$$

where $\zeta=\kappa-(\kappa-K)\exp(-s\tau)$. Equation (A7) has a solution only if the determinant of the coefficient matrix vanishes. Therefore, we obtain the following characteristic equation for the stability of the synchronization:

$$D(s)=s^3+[\gamma_R+2\zeta\cos(\omega_{\rm st}\tau)]s^2+[\omega_R^2+2\gamma_R\zeta\cos(\omega_{\rm st}\tau)+\zeta^2]s+\gamma_R\zeta^2+\omega_R^2\zeta[\cos(\omega_{\rm st}\tau)-\alpha\sin(\omega_{\rm st}\tau)]=0, \tag{A8}$$

where $\omega_R^2=G_N^2E_{\rm st}^2(N_{\rm st}-N_0)=\gamma_c G_N E_{\rm st}^2$ and $\gamma_R=\gamma_N+G_N E_{\rm st}^2$ represent an angular frequency and a decay rate for the relaxation oscillation of a solitary laser. Substituting $s=\gamma+i\omega$, Eq. (A8) is seen to have a large number of linear modes as pairs of γ and ω [8].

[1] T. Yamada and H. Fujisaka, Prog. Theor. Phys. **70**, 1240 (1983); **72**, 885 (1984); R. V. Jensen, Phys. Rev. E **58**, R6907 (1998).
[2] L. M. Pecora and T. L. Carroll, Phys. Rev. Lett. **64**, 821 (1990); Phys. Rev. A **44**, 2374 (1991).
[3] K. M. Cuomo and A. V. Oppenheim, Phys. Rev. Lett. **71**, 65 (1993).
[4] G. Perez and H. A. Cerdeira, Phys. Rev. Lett. **74**, 1970 (1995).
[5] K. Pyragas, Phys. Rev. E **58**, 3067 (1998).
[6] R. Lang and K. Kobayashi, IEEE J. Quantum Electron. **16**, 347 (1980).
[7] A. Masoller and N. B. Abraham, Phys. Rev. A **57**, 1313 (1998).
[8] A. Murakami and J. Ohtsubo, IEEE J. Quantum Electron. **34**, 1979 (1998).
[9] S.-Y. Ye and J. Ohtsubo, Op. Rev. **5**, 280 (1998); A. Murakami and J. Ohtsubo, *ibid.* **6**, 359 (1999).
[10] Y. Ikuma and J. Ohtsubo, IEEE J. Quantum Electron. **34**, 1240 (1998).
[11] G. H. M. Tartwijk and G. P. Agrawal, Prog. Quantum Electron. **22**, 43 (1998).
[12] J. Ohtsubo, Opt. Rev. **6**, 1 (1999).
[13] R. Roy and K. S. Thornburg, Jr., Phys. Rev. Lett. **72**, 2009 (1994).
[14] T. Sugawara, M. Tachikawa, T. Tsukamoto, and T. Shimizu, Phys. Rev. Lett. **72**, 3502 (1994).
[15] H. D. I. Abarbanel and M. B. Kennel, Phys. Rev. Lett. **80**, 3153 (1998).
[16] D. Y. Tang, R. Dykstra, M. W. Hamilton, and N. R. Heckenberg, Phys. Rev. E **57**, 5247 (1998).
[17] C. L. Pando, Phys. Rev. E **57**, 2725 (1998).
[18] P. Colet and R. Roy, Opt. Lett. **19**, 2056 (1994).
[19] V. Annovazzi-Lodi, S. Donati, and A. Scire, IEEE J. Quantum Electron. **32**, 953 (1996).
[20] G. D. VanWiggeren and R. Roy, Science **279**, 1198 (1998).
[21] A. Uchida, T. Ogawa, M. Shinozuka, and F. Kannari, Phys. Rev. E **62**, 1 (2000).
[22] J.-P. Goedgebuer, L. Larger, and H. Porte, Phys. Rev. Lett. **80**, 2249 (1998).
[23] C. R. Mirasso, P. Colet, and P. Garcia-Fernandez, IEEE Photonics Technol. Lett. **8**, 299 (1996).
[24] V. Annovazzi-Lodi, S. Donati, and A. Scire, IEEE J. Quantum Electron. **33**, 1449 (1997).
[25] V. Ahlers, U. Parlitz, and W. Lauterborn, Phys. Rev. E **58**, 7208 (1998).
[26] Y. Takiguchi, H. Fujino, and J. Ohtsubo, Opt. Lett. **24**, 1570 (1999).
[27] I. Fischer, Y. Liu, and P. Davis, Phys. Rev. A **62**, 011801(R) (2000).
[28] Y. Liu, H. F. Chen, J. M. Liu, P. Davis, and T. Aida, Phys. Rev. A (to be published).
[29] H. Fujino and J. Ohtsubo, Opt. Lett. **25**, 625 (2000).
[30] L. Rahman, G. Li, and F. Tian, Opt. Commun. **15**, 91 (1997).
[31] H. F. Chen and J. M. Liu, IEEE J. Quantum Electron. **36**, 27 (2000).
[32] K. Pyragas, Phys. Lett. A **181**, 203 (1993); **170**, 421 (1992).
[33] K. Murali and M. Lakshmanan, Phys. Rev. E **49**, 4882 (1994); T. Kapitaniak, *ibid.* **50**, 1642 (1994).
[34] H. U. Voss, Phys. Rev. E **61**, 5115 (2000).